Supporting Information

Oxygen-Atom Transfer Reactivity of Axially Ligated Mn(V)–Oxo Complexes: Evidence for Enhanced Electrophilic and Nucleophilic Pathways

Heather M. Neu, Tzuhsiung Yang, Regina A. Baglia, Timothy H. Yosca, Michael T. Green*, Matthew G. Quesne, Sam P. de Visser*, David P. Goldberg*

Computational Methods. Computational studies on the binding of different axial ligands to $^{1}[(H_8Cz)Mn^{V}(O)]$ were performed using the *Orca* program package.[1] The resolution of identity (RIJ) and the chain-of-sphere (COSX) approximations[2,3] on the Coulomb and the exchange correlation, respectively, with auxiliary basis sets that corresponded to the basis sets of atoms were used throughout the studies. Geometry optimizations and frequency calculations were performed using hybrid density functional theory B3LYP[4,5] with the non-relativistic effective core potential basis set LANL2DZ[6] from the Los Alamos National Laboratory to the double-ζ quality on the Mn and the split-valence double- ζ basis set 6-31G[7] on the remaining atoms. Initial geometry of the manganese-oxo corrolazine $^{1}[(TBP_8Cz)Mn^{V}(O)]$ was obtained from the X-ray crystal structure of the manganese-imido corrolazine complex[8] $(TBP_8Cz)Mn^{V}(NMes)$ (Mes = mesityl) by replacing the imido ligand with an oxo ligand and the *p-tert*-butylphenyl groups with hydrogens. Subsequent calculations on the axially-ligated complexes $^{1}[(H_8Cz)Mn^{V}(O)(X)]^{-}$, where X = F^{-}, CN^{-}, OCN^{-}, N_3^{-}, NO_3^{-}, were achieved by manually adding the corresponding ligands to the manganese complex and then allowing the structures to optimize without constraints. Optimized geometries were used for frequency calculations at the same level of theory to ensure the local minimum nature of the geometry (without any imaginary frequencies).

References:

(1) Neese, F. *Wiley Interdiscip. Rev.: Comput. Mol. Sci.* **2012**, *2*, 73-78.
(2) Neese, F.; Wennmohs, F.; Hansen, A.; Becker, U. *Chem. Phys.* **2009**, *356*, 98-109.
(3) Kendall, R. A.; Fruchtl, H. A. *Theor. Chem. Acc.* **1997**, *97*, 158-163.
(4) Becke, A. D. *J. Chem. Phys.* **1993**, *98*, 5648-5652.
(5) Lee, C. T.; Yang, W. T.; Parr, R. G. *Phys. Rev. B* **1988**, *37*, 785-789.
(6) Hay, P. J.; Wadt, W. R. *J. Chem. Phys.* **1985**, *82*, 299-310.
(7) Hehre, W. J.; Ditchfie, R.; Pople, J. A. *J. Chem. Phys.* **1972**, *56*, 2257-2261.
(8) Lansky, D. E.; Kosack, J. R.; Sarjeant, A. A. N.; Goldberg, D. P. *Inorg. Chem.* **2006**, *45*, 8477-8479.

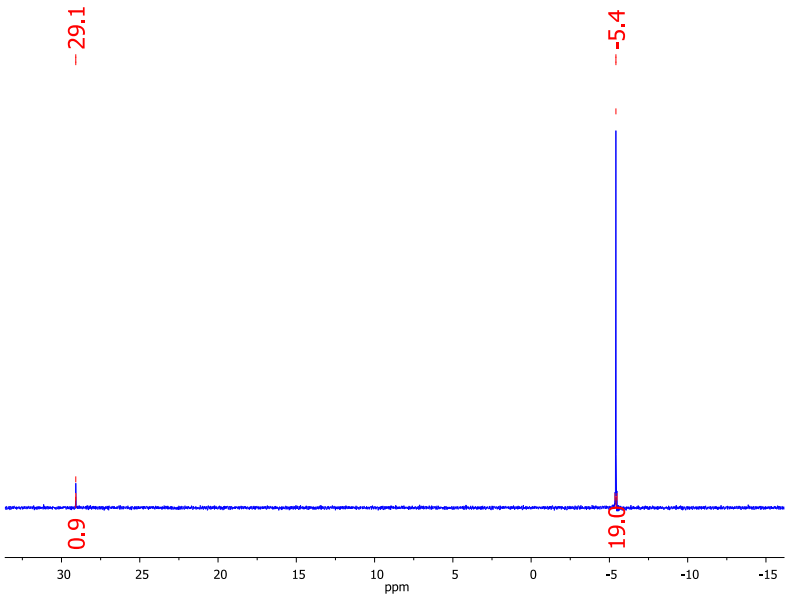

Figure S1. ^{31}P-NMR spectrum of the reaction of $[(TBP_8Cz)Mn^{V}(O)(F)]^{-}$ (0.25 mM) with PPh_3 (5.0 mM, -5.4 ppm) at 25 °C under argon to give $[(TBP_8Cz)Mn^{III}(F)]^{-}$ and $OPPh_3$ (29.1 ppm) in CH_2Cl_2. The reaction mixture was dried and redissolved in $CDCl_3$ prior to obtaining the spectrum.

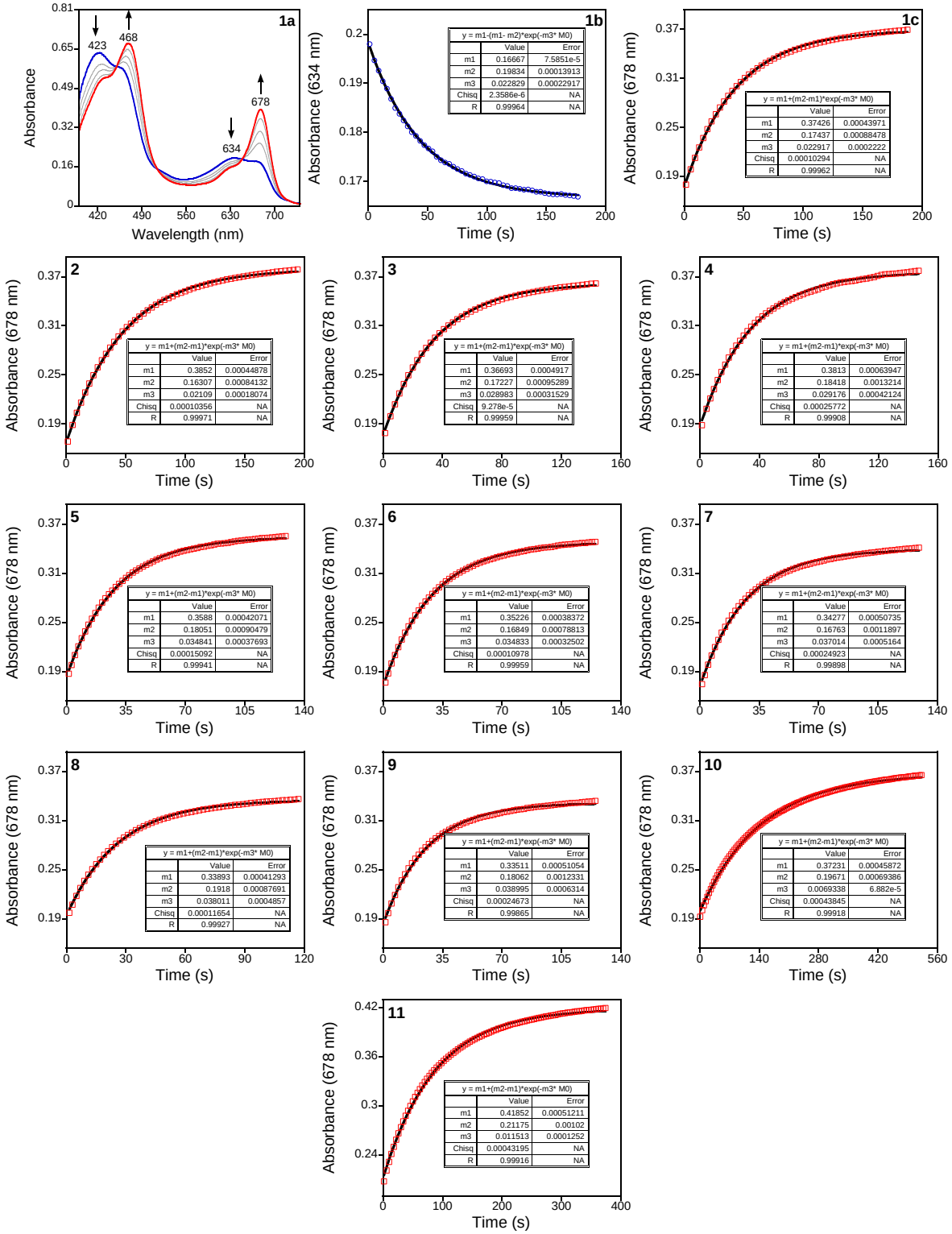

Figure S2. (1a) UV-vis spectral changes for the reaction of $(TBP_8Cz)Mn^{V}(O)$ (10 μM) (423, 634 nm) with $Bu_4N^+F^-{\cdot}3H_2O$ (13.5 mM) and DBS (2.7 mM) to give $[(TBP_8Cz)Mn^{III}(F)]^-$ (468, 678 nm) in CH_2Cl_2 at 25 °C. (1b) Changes in absorbance versus time for the decay of $[(TBP_8Cz)Mn^{V}(O)(F)]^-$ (634 nm) for the reaction of $(TBP_8Cz)Mn^{V}(O)$ (10 μM) with $Bu_4N^+F^-{\cdot}3H_2O$ (13.5 mM) and DBS (2.7 mM). (1c) Changes in absorbance versus time for the growth of $[(TBP_8Cz)Mn^{III}(F)]^-$ (678 nm) for the reaction of $(TBP_8Cz)Mn^{V}(O)$ (10 μM) with $Bu_4N^+F^-{\cdot}3H_2O$ (13.5 mM) and DBS (2.7 mM). (2-11) Changes in absorbance versus time for the growth of $[(TBP_8Cz)Mn^{III}(F)]^-$ (678 nm) for the reaction of $(TBP_8Cz)Mn^{V}(O)$ (10 μM) and DBS (2.7 mM) with varied concentrations of $Bu_4N^+F^-{\cdot}3H_2O$: (2) 8.4 mM, (3) 16.8 mM, (4) 25.2 mM, (5) 33.6 mM, (6) 37.0 mM, (7) 42.0 mM, (8) 50.4 mM, (9) 58.8 mM, (10) 1.7 mM, and (11) 3.4 mM.

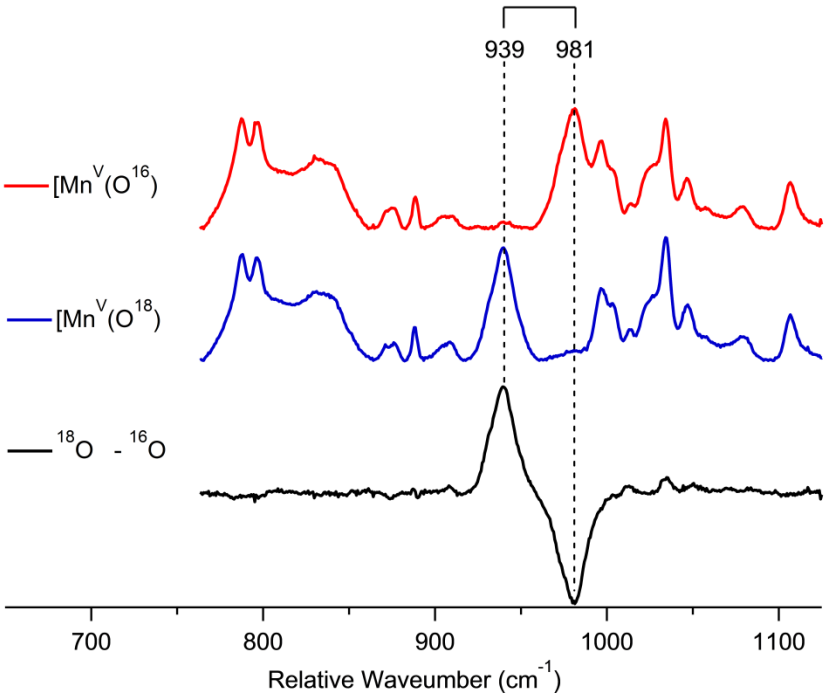

Figure S3. Low frequency resonance Raman spectra of $^{16}O/^{18}O$ $(TBP_8Cz)Mn^V(O)$. The resonances near 900 cm^{-1} were used to scale the spectra. Data were collected using a 413.2 nm krypton-ion laser line.

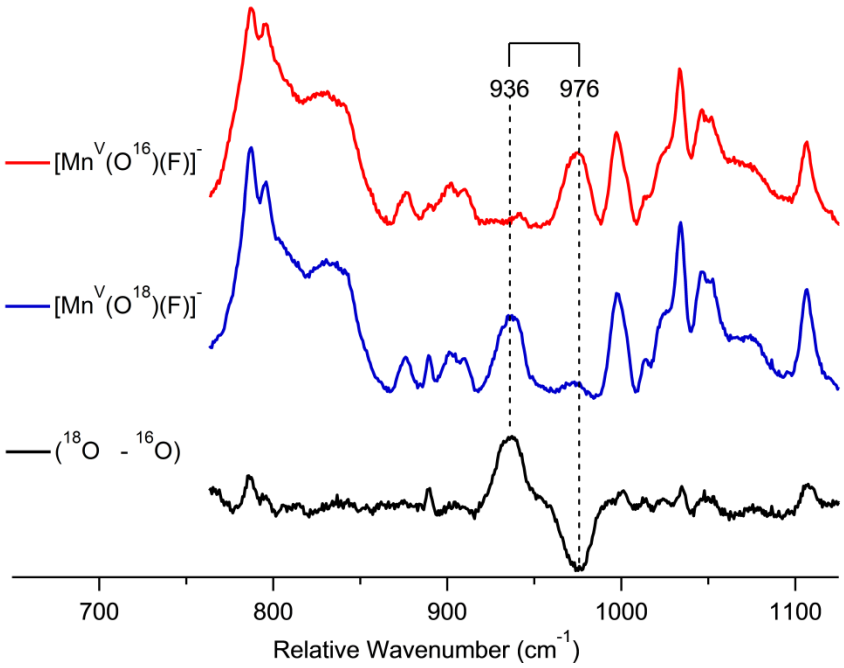

Figure S4. Low frequency resonance Raman spectra of $^{16}O/^{18}O$ $[(TBP_8Cz)Mn^V(O)(F)]^-$. The resonances near 900 cm^{-1} were used to scale the spectra. Data were collected using a 413.2 nm krypton-ion laser line.

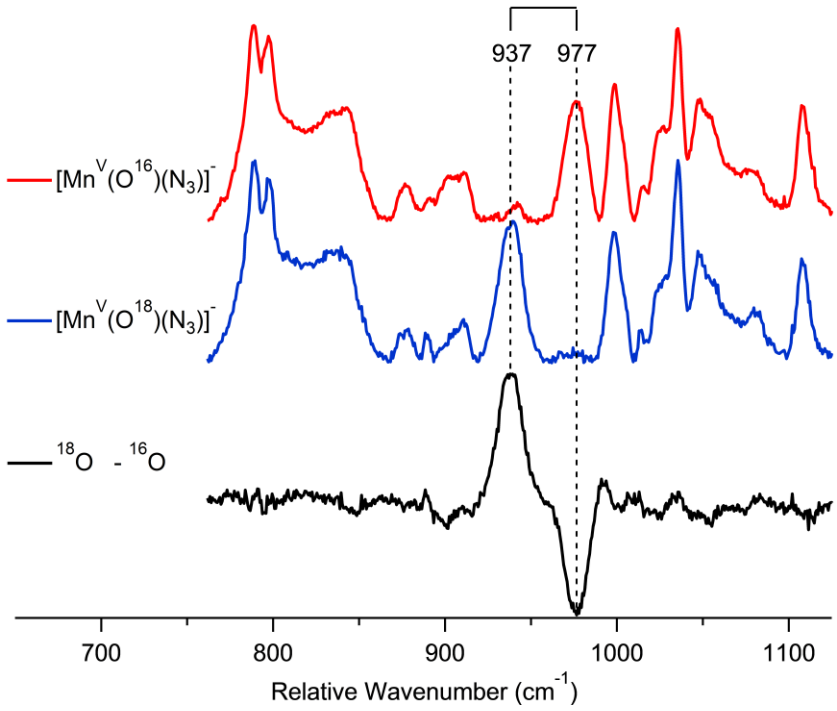

Figure S5. Low frequency resonance Raman spectra of $^{16}O/^{18}O$ $[(TBP_8Cz)Mn^{V}(O)(N_3)]^{-}$. The resonances near 900 cm^{-1} were used to scale the spectra. Data were collected using a 413.2 nm krypton-ion laser line.

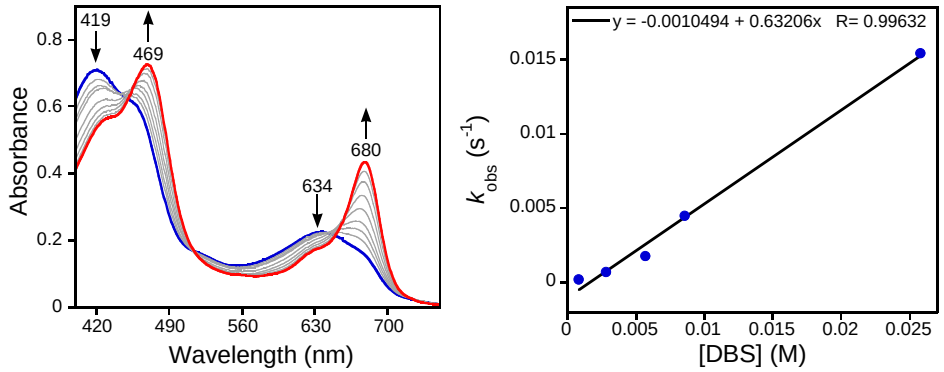

Figure S6. (Left) Time-resolved UV-vis spectra of the reaction of $[(TBP_8Cz)Mn^{V}(O)(F)]^{-}$ (12.7 μM) (419, 634 nm) (blue line) with DBS (0.86 mM) at 25 °C under argon to give $[(TBP_8Cz)Mn^{III}(F)]^{-}$ (469, 680 nm) (red line) in CH_2Cl_2. (Right) Plot of k_{obs} versus concentration of DBS.

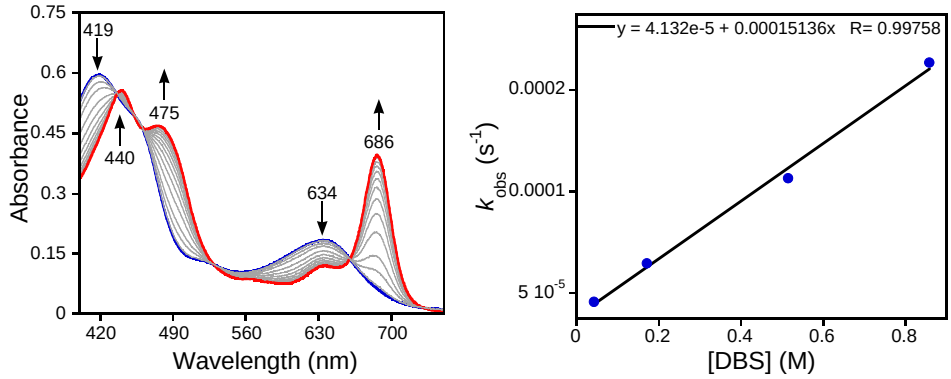

Figure S7. (Left) Time-resolved UV-vis spectra of the reaction of $(TBP_8Cz)Mn^{V}(O)$ (11.5 μM) (419, 634 nm) with NBu_4SCN (11.5 mM) and DBS (0.86 M) to give $[(TBP_8Cz)Mn^{III}(SCN)]^{-}$ (440, 475, 686 nm) in CH_2Cl_2 at 25 °C. (Right) Plot of k_{obs} versus concentration of DBS.

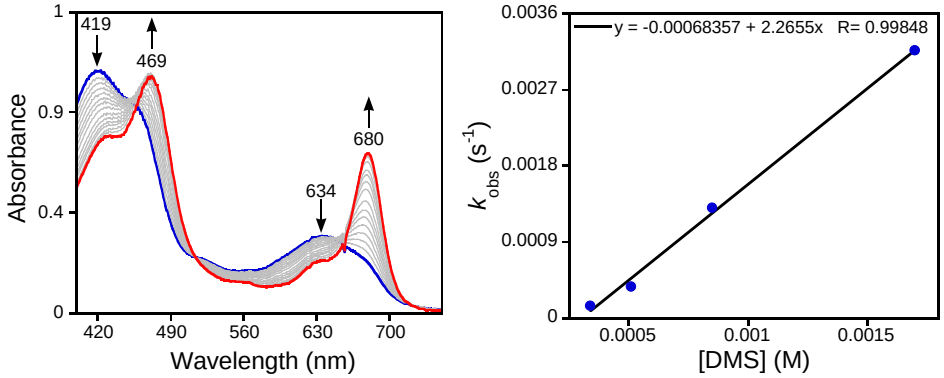

Figure S8. (Left) Time-resolved UV-vis spectra of the reaction of $[(TBP_8Cz)Mn^{V}(O)(F)]^{-}$ (14.9 μM) (419, 634 nm) (blue line) with DMS (0.34 mM) at 25 °C under argon to give $[(TBP_8Cz)Mn^{III}(F)]^{-}$ (469, 680 nm) (red line) in CH_2Cl_2. (Right) Plot of k_{obs} versus concentration of DMS.

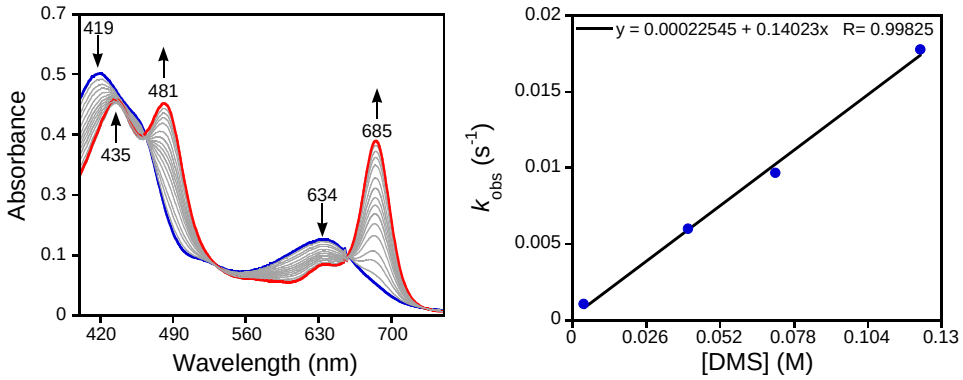

Figure S9. (Left) Time-resolved UV-vis spectra of the reaction of $[(TBP_8Cz)Mn^{V}(O)(N_3)]^-$ (11.5 μM) (419, 634 nm) with DMS (4.0 mM) to give $[(TBP_8Cz)Mn^{III}(N_3)]^-$ (435, 481, 685 nm) in CH_2Cl_2 at 25 °C. (Right) Plot of k_{obs} versus concentration of DMS.

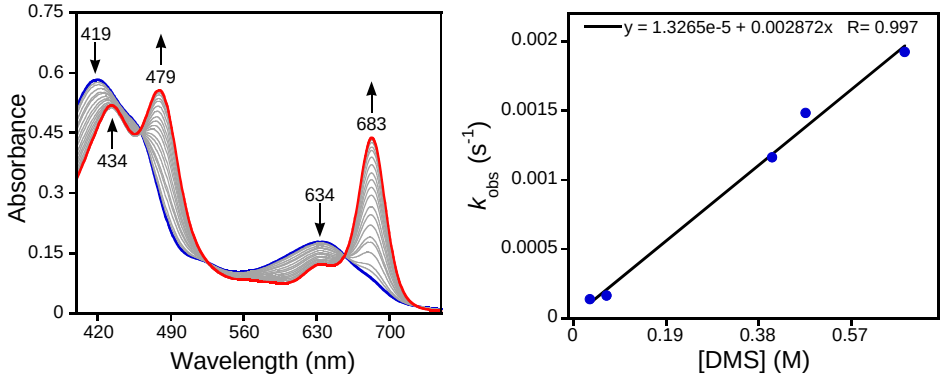

Figure S10. (Left) Time-resolved UV-vis spectra of the reaction of $[(TBP_8Cz)Mn^{V}(O)(OCN)]^-$ (11.6 μM) (419, 634 nm) with DMS (0.4 M) to give $[(TBP_8Cz)Mn^{III}(OCN)]^-$ (434, 479, 683 nm) in CH_2Cl_2 at 25 °C. (Right) Plot of k_{obs} versus concentration of DMS.

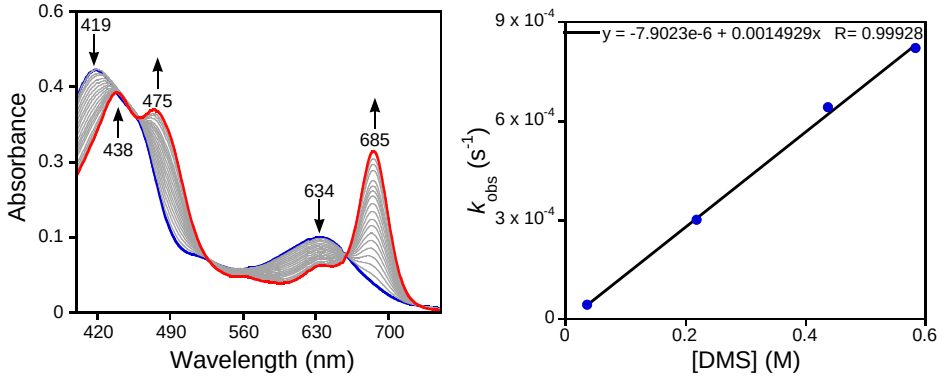

Figure S11. (Left) Time-resolved UV-vis spectra of the reaction of $[(TBP_8Cz)Mn^{V}(O)(NO_3)]^-$ (9.6 μM) (419, 634 nm) with DMS (0.54 M) to give $[(TBP_8Cz)Mn^{III}(NO_3)]^-$ (438, 475, 685 nm) in CH_2Cl_2 at 25 °C. (Right) Plot of k_{obs} versus concentration of DMS.

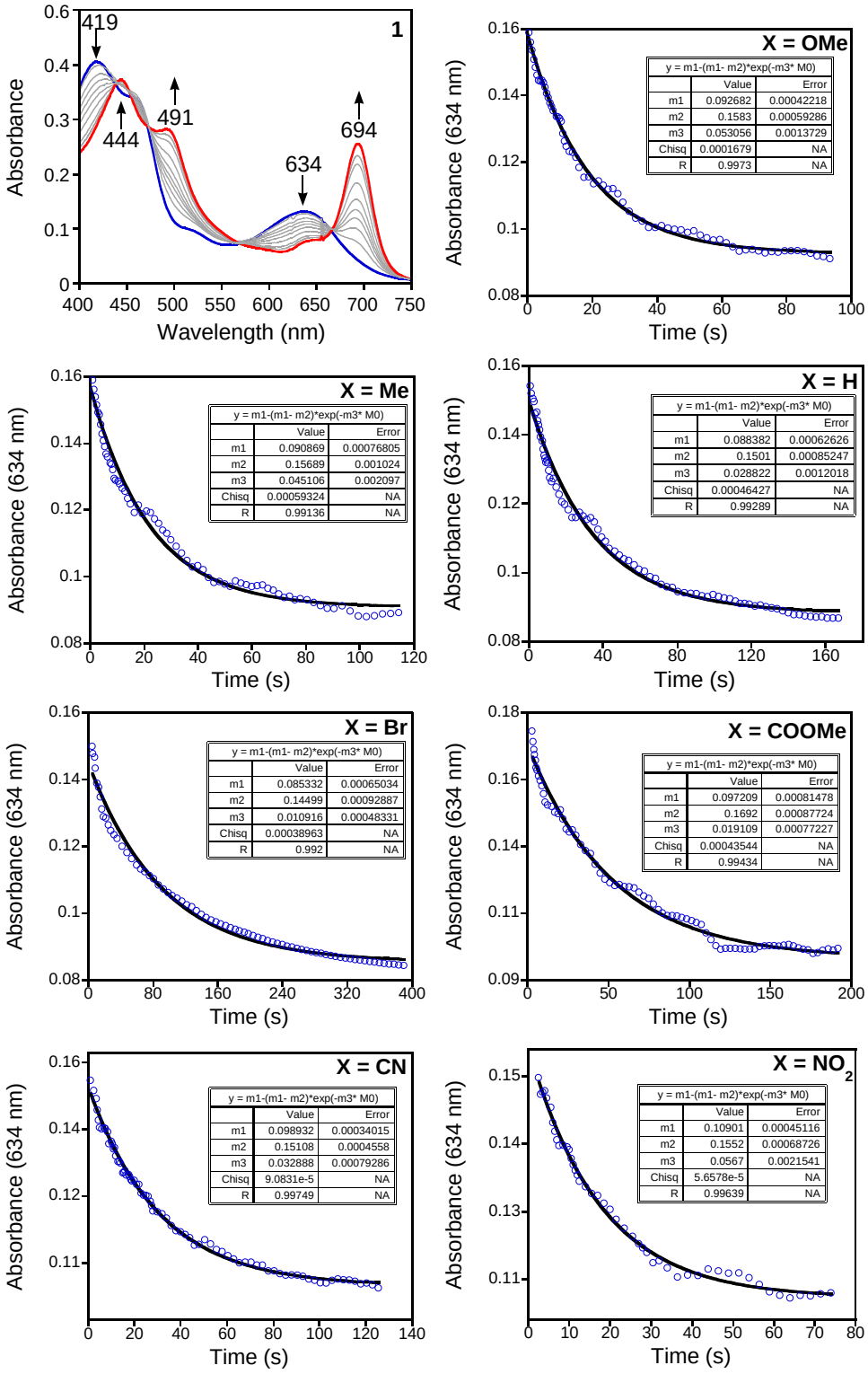

Figure S12. (1) Representative UV-vis spectral changes for the reaction of $(TBP_8Cz)Mn^{V}(O)$ (12 μM) (419, 634 nm) with $Bu_4N^{+}CN^{-}$ (12 mM) and methyl 4-(methylthio)benzoate (0.13 M) to give $[(TBP_8Cz)Mn^{III}(CN)]^{-}$ (444, 491, 694 nm) in toluene at 25 °C. Representative changes in absorbance versus time for the decay of $[(TBP_8Cz)Mn^{V}(O)(CN)]^{-}$ (634 nm) with different *para*-X-substituted thioanisoles.

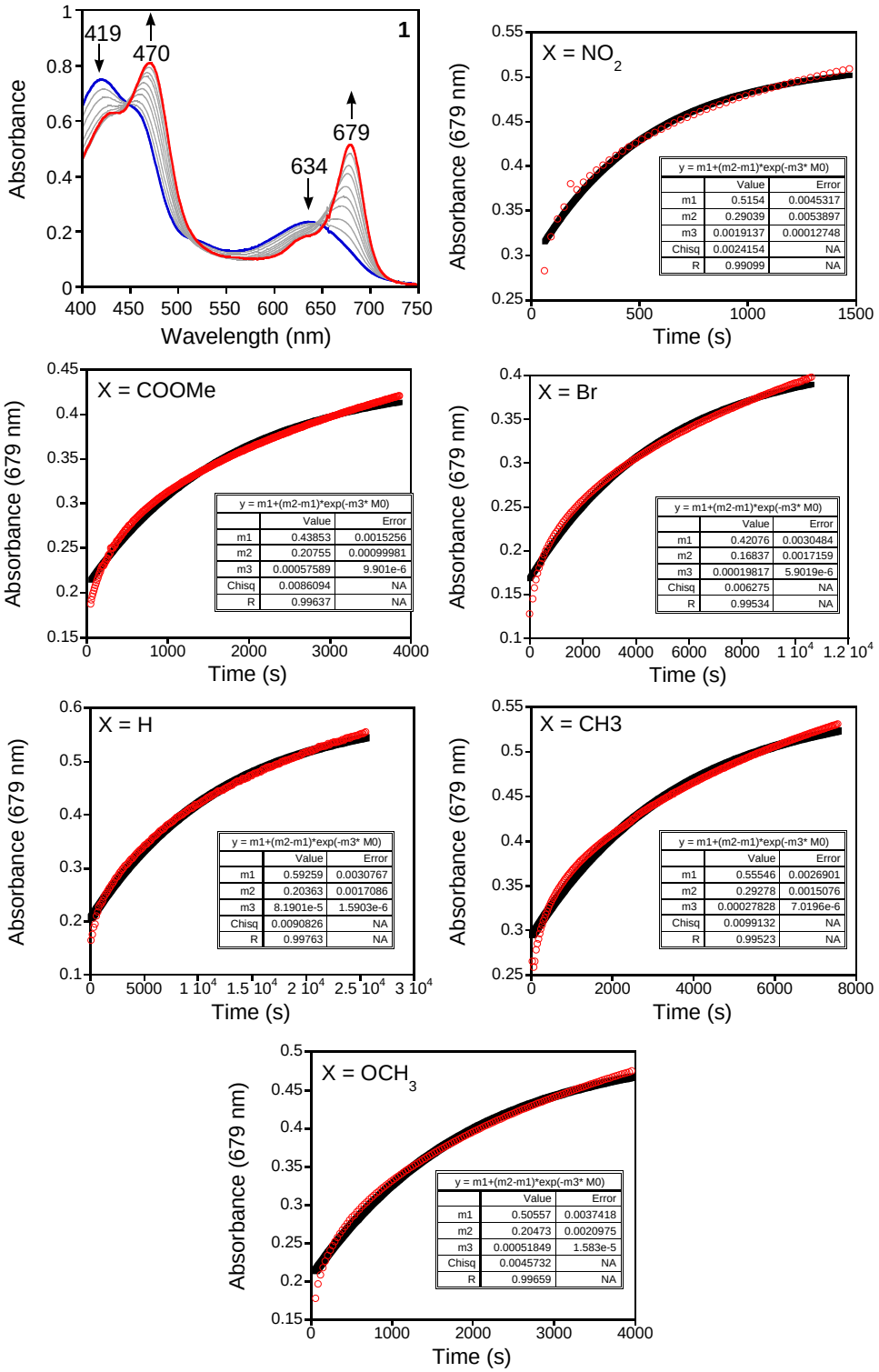

Figure S13. (1) Representative UV-vis spectral changes for the reaction of $(TBP_8Cz)Mn^{V}(O)$ (15 μM) (419, 634 nm) with $Bu_4N^+F^-$ (15 mM) and methyl 4-(methylthio)benzoate (0.13 M) to give $[(TBP_8Cz)Mn^{III}(F)]^-$ (470, 679 nm) in CH_2Cl_2 at 25 °C. Representative changes in absorbance versus time for the growth of $[(TBP_8Cz)Mn^{III}(F)]^-$ (679 nm) with different *para*-X-substituted thioanisoles.

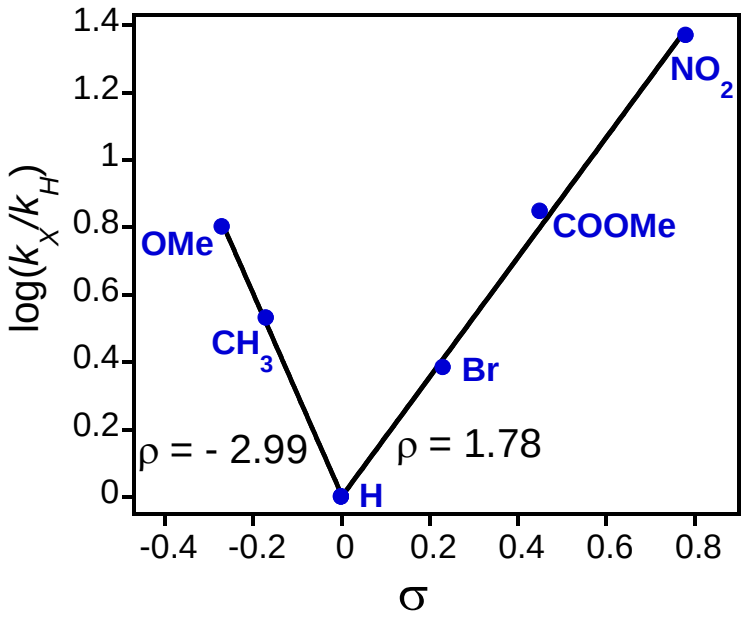

Figure S14. Hammett plot for the reaction of $[Mn^{V}(O)(TBP_8Cz)(F)]^{-}$ and *para*-X-substituted thioanisole derivatives.

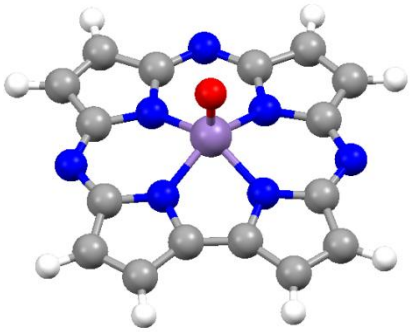

r_{MnO} = 1.549
ΔMn = 0.57

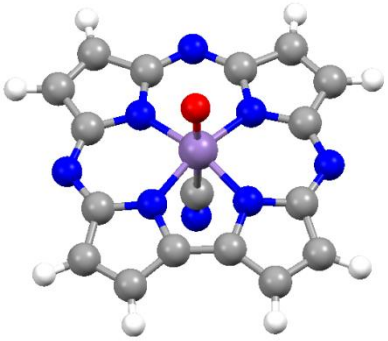

r_{MnO} = 1.568
$r_{Mn(CN)}$ = 2.146
ΔMn = 0.30

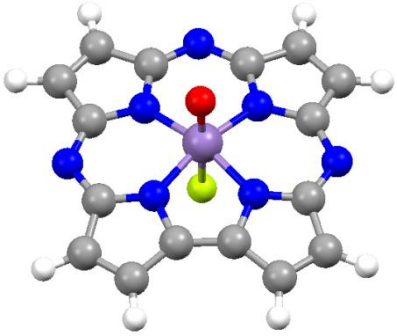

r_{MnO} = 1.568
$r_{Mn(F)}$ = 1.931
ΔMn = 0.27

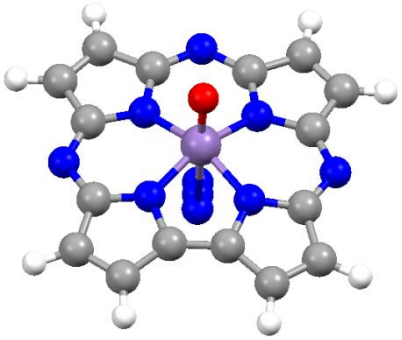

r_{MnO} = 1.568
$r_{Mn(N_3)}$ = 2.354
ΔMn = 0.37

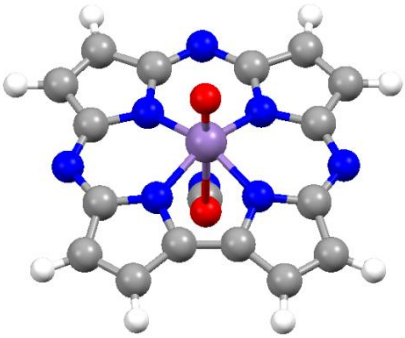

r_{MnO} = 1.561
$r_{Mn(OCN)}$ = 2.420
ΔMn = 0.41

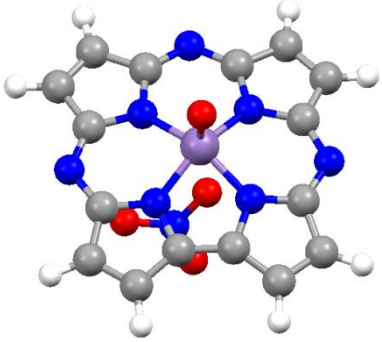

r_{MnO} = 1.557
$r_{Mn(NO_3)}$ = 2.518
ΔMn = 0.46

Figure S15. Optimized geometries of $^1[(H_8Cz)Mn^V(O)(X)]^-$ (X = no ligand, CN^-, F^-, N_3^-, OCN^-, and NO_3^-) with Mn-O bond distance (r_{MnO}), Mn-X bond distance (r_{MnX}) and Mn-Cz out-of-plane displacement (plane defined by the four internal nitrogens) (ΔMn) shown in angstroms.

Table S1. Selected calculated molecular parameters for $^{1}[(H_8Cz)Mn^{V}(O)(X)]^{-}$ (X = no ligand, CN^{-}, F^{-}, N_3^{-}, OCN^{-}, and NO_3^{-}) in angstroms.

X	—	CN^{-}	F^{-}	N_3^{-}	OCN^{-}	NO_3^{-}
Mn-O	1.549	1.568	1.568	1.568	1.561	1.557
$Mn\text{-}N^{eq}_{ave}$	1.884(10)	1.894(17)	1.89(2)	1.89(3)	1.884(14)	1.882(12)
ΔMn	0.57	0.30	0.270	0.37	0.41	0.46
Mn-X	—	2.146	1.931	2.354	2.420	2.518

Cartesian coordinates of all optimized geometries reported here:

Axial ligand binding to ^{1}[(H$_8$Cz)Mn^V(O)]

^{1}[(H$_8$Cz)Mn^V(O)]:

Mn	-0.128223	0.019262	-0.051263
N	0.572893	-1.344946	-1.161183
C	0.226823	-2.711893	-1.120290
N	-0.331538	-3.365152	-0.097092
C	-0.595430	-2.713402	1.040156
N	-0.402450	-1.350465	1.200202
C	-0.665443	-0.997130	2.520104
C	-0.365131	0.356182	2.734985
N	0.103977	0.945792	1.564173
C	0.526000	2.237538	1.837312
N	1.139014	3.018505	0.942321
C	1.435238	2.529864	-0.266157
N	1.151837	1.235080	-0.747515
C	1.749486	1.124578	-2.013166
N	1.766947	0.032921	-2.777234
C	1.235979	-1.121464	-2.376948
C	1.273642	-2.358423	-3.113868
C	0.654862	-3.320256	-2.355774
H	0.508493	-4.364066	-2.587415
H	1.728531	-2.459719	-4.086751
C	2.379501	2.379222	-2.334916
C	2.186678	3.231408	-1.276059
H	2.541945	4.242992	-1.154946
H	2.908834	2.562164	-3.257098
C	0.252163	2.487902	3.225734
C	-0.287837	1.331112	3.776947
H	-0.584105	1.176321	4.803780
H	0.465493	3.420028	3.726298
C	-1.081819	-2.177547	3.212403
C	-1.044867	-3.229188	2.305845
H	-1.297565	-4.261789	2.492402
H	-1.366253	-2.235457	4.252255
O	-1.500010	0.393341	-0.663699

^{1}[(Cz)Mn^V(O)(CN)]$^-$:

Mn	-0.035603	0.011127	-0.005671
N	1.898547	0.009667	-0.061817
C	2.706945	1.131651	-0.035708
N	2.320479	2.414741	-0.126826
C	1.019296	2.750141	-0.280128
N	-0.023437	1.858454	-0.266230
C	-1.220363	2.471985	-0.605027
C	-2.255082	1.518471	-0.785902
N	-1.799012	0.222920	-0.552684
C	-2.738210	-0.707458	-0.932168
N	-2.525802	-2.043216	-0.960640
C	-1.311102	-2.558528	-0.716448
N	-0.153178	-1.864084	-0.400088
C	0.922900	-2.721030	-0.361692
N	2.217669	-2.397979	-0.188681
C	2.658960	-1.131449	-0.070385
C	4.056474	-0.716792	0.006228
C	4.084658	0.655853	0.029605
H	4.942468	1.311086	0.061413
H	4.886396	-1.407601	0.024478
C	0.408735	-4.063395	-0.606253
C	-0.944660	-3.963928	-0.819565
H	-1.647237	-4.748245	-1.059070
H	1.029000	-4.947298	-0.624353
C	-3.899622	0.037181	-1.343246
C	-3.598570	1.399914	-1.262039
H	-4.248509	2.217584	-1.538045
H	-4.821051	-0.409200	-1.687610
C	-0.933200	3.867940	-0.764366
C	0.435445	4.041573	-0.554963
H	0.992557	4.965529	-0.608290
H	-1.646283	4.637160	-1.022777
O	-0.017076	-0.186745	1.559566
C	0.307611	0.032707	-2.124340
N	0.511871	0.023145	-3.289851

^{1}[(Cz)Mn^V(O)(F)]$^-$:

Mn	0.167041	-0.051576	0.077626
N	0.660239	-1.401232	-1.187966
C	0.352721	-2.751931	-1.084857
N	-0.184556	-3.392444	-0.034643
C	-0.498436	-2.736673	1.108755
N	-0.433457	-1.380471	1.262635
C	-0.647163	-1.006252	2.576501
C	-0.352356	0.366626	2.791344
N	0.064762	0.996038	1.628194
C	0.604753	2.226016	1.898936
N	1.269053	2.989261	0.999003
C	1.552394	2.531171	-0.229127
N	1.222976	1.292879	-0.771700
C	1.844764	1.130712	-1.989058
N	1.869794	0.019988	-2.749484
C	1.332239	-1.150300	-2.357975
C	1.418165	-2.412982	-3.083431
C	0.820928	-3.380518	-2.314774
H	0.712134	-4.432969	-2.533594
H	1.890602	-2.522825	-4.048339
C	2.553468	2.370913	-2.280548
C	2.378044	3.216180	-1.212455
H	2.787440	4.205071	-1.066452
H	3.122870	2.541699	-3.182549
C	0.423240	2.446964	3.313695
C	-0.156365	1.300781	3.860952
H	-0.394423	1.127223	4.901477
H	0.726184	3.342464	3.837152
C	-0.946591	-2.209106	3.302714
C	-0.866630	-3.270685	2.403666
H	-1.033189	-4.316197	2.620581
H	-1.181183	-2.276852	4.355871
O	-1.179014	0.281546	-0.655381
F	1.887297	-0.525920	0.814540

^{1}[(Cz)Mn^V(O)(OCN)]$^-$:

Mn	-0.003531	0.008744	0.080764
N	1.876594	0.028058	-0.172027
C	2.701258	1.159473	-0.126966
N	2.324721	2.440337	-0.168267
C	1.019196	2.764446	-0.267736
N	-0.005129	1.857844	-0.206148
C	-1.214948	2.467687	-0.503367
C	-2.243259	1.516979	-0.674689
N	-1.781342	0.222224	-0.469937
C	-2.713606	-0.687954	-0.898524
N	-2.498641	-2.016491	-0.977967
C	-1.276335	-2.513457	-0.775336
N	-0.107368	-1.801188	-0.471514
C	0.963482	-2.682012	-0.470895
N	2.253568	-2.373487	-0.293617
C	2.671415	-1.105355	-0.196982
C	4.055541	-0.680091	-0.122329
C	4.072890	0.691740	-0.081481
H	4.924040	1.354997	-0.051141
H	4.888231	-1.366966	-0.124545
C	0.445912	-4.012104	-0.724486
C	-0.910009	-3.908364	-0.910992
H	-1.617457	-4.684546	-1.160986
H	1.069240	-4.891738	-0.778842
C	-3.876183	0.061054	-1.299492
C	-3.582660	1.417244	-1.166397
H	-4.224148	2.245226	-1.430253
H	-4.788902	-0.382827	-1.668773
C	-0.952980	3.865157	-0.672138
C	0.419148	4.051266	-0.519144
H	0.969678	4.977322	-0.593292
H	-1.685292	4.622908	-0.908891
O	-0.068159	-0.120390	1.634693
O	0.065776	0.300425	-2.320676
C	0.803415	-0.403288	-3.078472
N	1.493550	-1.062669	-3.800522

^{1}[(Cz)Mn^V(O)(N$_3$)]$^-$:

Mn	-0.009136	0.020689	0.017112
N	1.890962	0.041965	-0.190950
C	2.705531	1.169344	-0.137857
N	2.319864	2.451619	-0.175085
C	1.012437	2.777236	-0.264996
N	-0.019445	1.874280	-0.195397
C	-1.230446	2.486085	-0.490476
C	-2.260667	1.532499	-0.669414
N	-1.794220	0.237239	-0.483480
C	-2.724451	-0.679711	-0.909293
N	-2.507168	-2.009730	-0.991455
C	-1.283139	-2.516660	-0.793927
N	-0.115485	-1.813120	-0.511779
C	0.955415	-2.683975	-0.483757
N	2.247688	-2.364433	-0.308526
C	2.673640	-1.095248	-0.207475
C	4.062874	-0.670914	-0.128667
C	4.081584	0.701185	-0.089953
H	4.934116	1.362925	-0.055061
H	4.896576	-1.356923	-0.125289
C	0.435952	-4.022576	-0.717959
C	-0.919742	-3.919677	-0.908381
H	-1.628284	-4.700673	-1.140493
H	1.056088	-4.905733	-0.752333
C	-3.892695	0.070492	-1.294935
C	-3.602526	1.428420	-1.155022
H	-4.252761	2.254373	-1.404779
H	-4.808334	-0.370866	-1.660426
C	-0.962088	3.881568	-0.662859
C	0.412965	4.064456	-0.514139
H	0.963628	4.990089	-0.596070
H	-1.690905	4.643780	-0.897560
O	-0.008515	-0.244016	1.562736
N	0.127902	0.261847	-2.320954
N	0.853498	-0.437477	-3.004912
N	1.546992	-1.098159	-3.707556

^{1}[(Cz)Mn^V(O)(NO$_3$)]$^-$:

Mn	-0.164193	0.046714	-0.076005
N	0.415663	-1.293892	-1.276335
C	0.098731	-2.658620	-1.205784
N	-0.441311	-3.314746	-0.177247
C	-0.671159	-2.671798	0.980407
N	-0.521725	-1.318411	1.149310
C	-0.721327	-0.970265	2.479180
C	-0.430284	0.388902	2.697034
N	-0.043741	1.019196	1.520019
C	0.441617	2.273428	1.790520
N	1.034118	3.067863	0.880688
C	1.291211	2.601848	-0.345312
N	0.974379	1.338351	-0.862478
C	1.582923	1.204294	-2.101969
N	1.608508	0.107718	-2.869350
C	1.084459	-1.055001	-2.465622
C	1.144843	-2.300898	-3.202030
C	0.535137	-3.268333	-2.444494
H	0.415568	-4.317796	-2.668106
H	1.612101	-2.401436	-4.169854
C	2.241116	2.455173	-2.414564
C	2.059975	3.303283	-1.350157
H	2.444908	4.302651	-1.214629
H	2.784862	2.632431	-3.330303
C	0.265055	2.492761	3.203792
C	-0.265399	1.331715	3.759945
H	-0.481897	1.146072	4.802226
H	0.538778	3.403201	3.715803
C	-1.076932	-2.166859	3.181367
C	-1.056443	-3.209610	2.261954
H	-1.267058	-4.251084	2.453989
H	-1.299899	-2.243929	4.235554
O	-1.558898	0.416815	-0.661383
N	2.730511	-1.344140	1.382328
O	3.664385	-1.157498	2.235440
O	2.164947	-0.285789	0.822396
O	2.337455	-2.521984	1.055508